Environmental Science & Technology

pubs.acs.org/est

Article

Particle-Bound Hg(II) is Available for Microbial Uptake as Revealed by a Whole-Cell Biosensor

Yuping Xiang, Yingying Guo, Guangliang Liu, Yanwei Liu, Maoyong Song, Jianbo Shi, Ligang Hu, Yongguang Yin,* Yong Cai, and Guibin Jiang

Cite This: *Environ. Sci. Technol.* 2022, 56, 6754−6764

Read Online

ACCESS | Metrics & More | Article Recommendations | Supporting Information

ABSTRACT: Particle-bound mercury (Hg_P), ubiquitously present in aquatic environments, can be methylated into highly toxic methylmercury, but it remains challenging to assess its bioavailability. In this study, we developed an *Escherichia coli*-based whole-cell biosensor to probe the microbial uptake of inorganic Hg(II) and assess the bioavailability of Hg_P sorbed on natural and model particles. This biosensor can quantitatively distinguish the contribution of dissolved Hg(II) and Hg_P to intracellular Hg. Results showed that the microbial uptake of Hg_P was ubiquitous in the environment, as evidenced by the bioavailability of sorbed-Hg(II) onto particulate matter and model particles (Fe_2O_3, Fe_3O_4, Al_2O_3, and SiO_2). In both oxic and anoxic environments, Hg_P was an important Hg(II) source for microbial uptake, with enhanced bioavailability under anoxic conditions. The composition of particles significantly affected the microbial uptake of Hg_P, with higher bioavailability being observed for Fe_2O_3 and lower for Al_2O_3 particles. The bioavailability of Hg_P varied also with the size of particles. In addition, coating with humic substances and model organic compound (cysteine) on Fe_2O_3 particles decreased the bioavailability of Hg_P. Overall, our findings highlight the role of Hg_P in Hg biogeochemical cycling and shed light on the enhanced Hg-methylation in settling particles and sediments in aquatic environments.

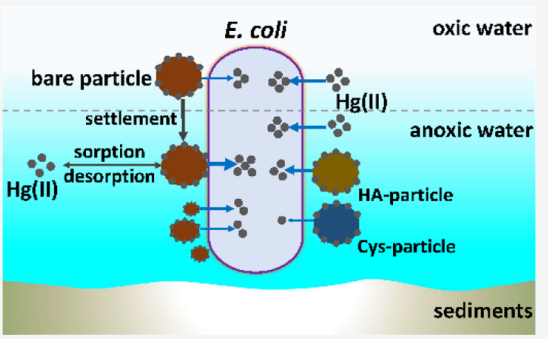

KEYWORDS: *natural particles, model particles, particle-bound Hg(II), bioavailability, whole-cell biosensor*

INTRODUCTION

Mercury (Hg) is a highly toxic pollutant with global distribution.[1] Of particular concern is methylmercury (MeHg), which is a neurotoxin that can bioaccumulate and biomagnify through food webs.[2,3] In aquatic environments, MeHg is primarily methylated from inorganic Hg(II) by anaerobic microorganisms, such as, sulfate-reducing bacteria, iron-reducing bacteria, and methanogens.[4,5] The methylation of Hg(II) is an intracellular process that is mainly affected by Hg(II) bioavailability and microbial activity.[6−8] In natural environments, the microbial uptake of Hg(II) is governed by its chemical speciation, which is largely affected by the complexation of Hg(II) with dissolved organic ligands[9,10] or its sorption to particles.[11,12] Therefore, knowledge regarding the microbial uptake of different Hg(II) species is important to predict the fate and ecological risks of Hg in aquatic environments.

In natural waters, a large amount of total Hg (THg) (approximately 20−95%) is bound with suspended particles, including inorganic minerals and particulate organic matter.[13−16] Traditionally, particles are considered as an important sink of Hg in aquatic ecosystems, considering the generally believed low bioavailability of particle-bound Hg(II) (Hg_P).[13,17] Recently, however, growing evidence has shown that Hg_P species are also available for microbial uptake and methylation, accounting an important source for aqueous MeHg in lakes and marine environments.[18−23] For instance, field studies have suggested that the Hg-methylation potential of settling particles are comparable to[24] or higher than[20] those of surface sediments and are probably mediated by anaerobic methylators in the anoxic microzones of particles.[25] Laboratory simulations further confirmed that Hg_P species could be taken up by Hg methylators, and methylation rates were significantly higher than Hg sulfide and even dissolved Hg(II) (Hg_D).[12,18] Considering the large storage of Hg_P in aquatic environments (e.g., in water column and sediment) and the rapid integration of MeHg generated from Hg_P into food webs,[26] clarifying the bioavailability of Hg_P is of critical importance for understanding the environmental fate and ecological risks of Hg.

Despite recent efforts to elucidate the microbial methylation of Hg_P,[27−31] the extent to which Hg_P species can be taken up

Received: December 30, 2021
Revised: April 2, 2022
Accepted: April 21, 2022
Published: May 3, 2022

by microorganisms is still largely unknown. This is because it is challenging to quantify and distinguish the contribution of Hg_P and Hg_D to bioavailable Hg pools. Conventionally, diffusive gradient thin film (DGT),[32] thiol-based extraction approach,[28] and Hg-methylation rate[12,18] were applied to assess the bioavailability of Hg(II). Although these methods work well in assessing Hg(II) bioavailability, the DGT method is not indicative of how Hg(II) crosses cell membranes in live cells, which may be subject to errors if macromolecular organic ligands and nanoparticulate dominate Hg(II) species.[33] The latter two methods can efficiently probe the Hg uptake by cells, but they are cumbersome and time-consuming in distinguishing the intracellular, microbial adsorbed Hg, and Hg_P, as well as in detecting Hg or MeHg. The whole-cell biosensor offers several advantages over these traditional methods in probing the transmembrane process and assessing the bioavailability of Hg(II). It can detect intracellular Hg in living cells in real-time without any pretreatment because it reflects bioavailable Hg fraction as fluorescent signals.[10,34−38] However, whether/how the whole-cell biosensor can be applied to assess the bioavailability of Hg_P remains unknown. In addition, it is unclear how surrounding redox conditions (i.e., oxic or anoxic niches) and the physicochemical properties of particles affect the microbial uptake of Hg_P species.

The objective of this study was to evaluate the role of particles in the microbial uptake of Hg(II). For this purpose, a whole-cell biosensor-based technique was developed for rapidly assessing the bioavailability of Hg_P under both oxic and anoxic conditions using both pure culture systems and filtered natural waters. We assayed the sorption of Hg(II) on natural particulate matter (PM), and used a Hg(II)-inducible and constitutive whole-cell biosensor to investigate the role of PM in controlling microbial Hg(II) uptake. We also explored how the physicochemical properties of particles affected Hg_P bioavailability using various model particles, including the composition, particle size, surface ligands, and particle concentration, and investigated the role of oxygen levels on Hg_P bioavailability by considering the transition from an oxic to an anoxic environment in a water column.

MATERIALS AND METHODS

Chemicals and Reagents. Natural soil PM was extracted from a peat soil from Changbai Mountain, China (42°9′51″N, 126°44′7″E), referred to Huang et al.,[39] to obtain two original PM (PM_{MCB1} and PM_{MCB2}), demineralized PM (demineralized PM_{MCB}), and ash fractions (ash PM_{MCB}). Natural aquatic PM was collected from the Yellow River (PM_{YR}, 113°33′48″ N, 34°57′3.6″ E) and Chaobai River, China (PM_{CBR}, 116°40′56″N, 40°9′54″E) in June 2021. Detailed extraction procedures and basic characteristics of PM are presented in the Supporting Information (SI 1 and Tables S1−S3). Model particles of various sizes, including Fe_2O_3 (17, 40, 95, and 166 nm), Fe_3O_4 (98, 189, and 227 nm), Al_2O_3 (14, 422, and 1065 nm), and SiO_2 (16, 373, and 2703 nm) were purchased from XiaoHuang Nano Technology (Shanghai, China). Their basic characteristics are presented in the Supporting Information (Figure S1 and Table S4).

Hg(II) standard solution [1000 mg Hg L^{-1} $Hg(NO_3)_2$, in 5% HNO_3] was obtained from Agilent (Palo Alto, CA). Humic acid (HA) and cysteine (Cys, 98%) were purchased from Alfa Aesar (Shanghai, China) and Sigma-Aldrich (St. Louis, MO) and were used as organic ligands to prepare organic matter-coated particles. 2,3-Dimercapto-1-propanesulfonic acid (DMPS, 95%), a strong Hg-chelating agent used to wash off Hg(II) adsorbed on cell surfaces,[28] was obtained from Aladdin (Shanghai, China). 3-(*N*-morpholino) propanesulfonic acid (MOPS, >99%), used to prepare the exposure buffer, was obtained from Sigma-Aldrich (St. Louis, MO). Other reagents used to prepare culture media were biochemical/analytical grade or higher and were obtained from Fisher Scientific (Waltham, MA) or Sinopharm Chemical Reagent (Shanghai, China). The ultrapure water (18.3 Ω) was prepared by a Milli-Q IQ700 system (Merck Millipore, Billerica, MA).

Construction and Cultivation of the Whole-Cell Biosensor. The Hg(II)-inducible biosensor (*Escherichia coli* PRL) that could probe intracellular Hg was designed based on previous reports.[34,37,40] The *merR* genes and pUC57 backbone for plasmid construction were the same as the literature,[34,37,40] but the *fbfp* reporter genes were replaced with the *luxCDABE* luminescence reporter genes because the luminescence signals of *luxCDABE* increased linearly with the increase in Hg(II) concentration,[41] and showed no significant difference under anoxic and oxic conditions.[42] Briefly, *merR* genes and a pUC57 backbone were commercially synthesized by Sangon Biotech (Shanghai, China). The *luxCDABE* genes were cloned from the pAKlux2 (P8513) plasmid (MiaolingBio, Wuhan, China). They were fused as the recombinant pUC57merR-*luxCDABE* plasmid, where the expression of *luxCDABE* genes occurred under the direct control of *merR* and was quantitatively induced by intracellular Hg(II).[35,38,43] Then, the constructed plasmid was transformed into *E. coli* DH5α (TransGen Biotech, Beijing, China), with plasmid selected/maintained by 100 μg mL^{-1} ampicillin (Amp) to obtain the biosensor strain *E. coli* PRL. Besides, a constitutive biosensor *E. coli* PJL, which contains a control plasmid (pUC57-J23106-*luxCDABE*) with luminescence emission as Hg(II)-independent, was developed to assess the effect of cell physiology on luminescence emission during exposure. The components of *E. coli* PJL were similar with those of *E. coli* PRL, but *merR* was replaced by the constitutive promoter BBa_J23106.[34] The long-term culture stocks of the biosensor strains were maintained in the LB medium with 100 μg mL^{-1} ampicillin and 30% sterile glycerol at −80 °C.

To initiate a biosensor assay, the stock strain was activated in anoxic/oxic LB broth at 30 °C overnight and then inoculated in anoxic-/oxic-modified MOPS buffer (MMOPS) at a 1% inoculation level at 30 °C. After growing to the mid-logarithmic growth stage (OD_{600} ≈ 0.6), cells were harvested by centrifugation (2350 g for 10 min) and then washed three times with fresh MMOPS before subsequent experiments. Ampicillin was added to a final concentration of 100 μg mL^{-1} in all media. For anoxic assays, fumarate (50 mM) was optimized as a limiting electron acceptor for exposure, and all handlings and incubations were conducted in an anaerobic glove chamber under an atmosphere of 80% N_2, 10% H_2, and 10% CO_2. For oxic assays, all handlings were conducted on a clean bench, and incubations were conducted in a shaker at 220 rpm. The detailed components of the LB broth and MMOPS buffer are supplied in the Supporting Information (SI 2).

Anoxic and Oxic Bioassays of Hg(II). The bioassay steps are present in Figure S2. For anoxic assays, the washed Hg(II)-inducible biosensor cells (*E. coli* PRL, OD_{600} = 0.4−0.5) were suspended with deoxygenated MMOPS to a final volume of 9.9 mL in 12 mL borosilicate glass vials. After 15 min pre-incubation, 0.1 mL of Hg(II) standards (100 times the final

https://doi.org/10.1021/acs.est.1c08946
Environ. Sci. Technol. 2022, 56, 6754−6764

concentration), freshly prepared from a 1000 mg Hg L^{-1} $Hg(NO_3)_2$ stock solution using MMOPS, was spiked in suspensions to initiate the bioassays. Samples were incubated at 30 °C in an anaerobic glove chamber. In 30 min intervals, 200 μL of samples from each vial were transferred into a sterile polystyrene 96-well microtiter plate (Costar, Corning Incorporated, Corning, NY), and the luminescence intensity in each well was analyzed using a Varioskan LUX microplate reader (v6.0.2.3, Thermo Scientific, Waltham, MA). Prior to luminescence analysis, samples in microplates were shaken at 240 rpm for 30 s to ensure the full aeration required for the luminescent reaction.[42,44] For oxic bioassays, sample preparation was conducted as described for the anoxic bioassays, but the MMOPS media were not deoxygenated, and all handlings were carried out on a clean bench. The integral time of luminescence analysis was 300 ms for anoxic and oxic assays. Simultaneously, the constitutive biosensor*E. coli*PJL was applied to assess the effect of cell phylogy on luminescence emissions. Three replicates were prepared for each treatment, and cell suspension without adding Hg(II) was set as a control. Meanwhile, the OD_{600} was monitored via a microplate reader to evaluate cell growth throughout the bioassays.

Additionally, to characterize the relationship between intracellular Hg(II) and luminescence intensity, Hg(II)-inducible biosensor cells (*E. coli* PRL) were exposed to 0−200 μg L^{-1} Hg(II) under anoxic conditions. Meanwhile, cells exposed to 20 μg L^{-1} Hg(II) under oxic conditions were used for comparison. After 3 h, an aliquot (200 μL) was used to analyze the luminescence intensity (see above). The remaining aliquot was centrifuged (2350 g for 10 min) to collect the cell pellets, and the cell surface adsorbed Hg(II) was washed off using 2 mL of 100 μM DMPS (100 rpm, 40 °C for 30 min).[28] Then, the washed cell pellets were suspended in 10 mM MMOPS for intracellular Hg analysis using a direct mercury analyzer (DMA-80, Milestone, Italy).[45]

Bioavailability Assays of Hg(II) Sorbed onto Natural Particulate Matter. The effect of natural particles on Hg(II) bioavailability was studied using the isolated PM. Before batch experiments, luminescence of the biosensor (*E. coli* PRL) induced by 0−50 μg L^{-1} Hg(II) in filtered river water (from CBR or YR) was measured to ensure that the biosensor could operate under oligotrophic conditions. The experimental conditions were similar to the oxic bioassays of dissolved Hg(II), but the MMOPS exposure buffer was replaced with unprocessed filtered river water (CBR or YR). The characteristics of the filtered river water are present in Table S2.

To investigate the bioavailability of Hg_P, the natural PM (Table S1) was initially suspended in corresponding filtered river water with a particle concentration of 0.1 g L^{-1} in 12 mL borosilicate glass vials. Due to the absence of soil PM (MCB) corresponding water, filtered CBR water was used instead. An aliquot of Hg(II) stock solution was added to each vial, reaching a final Hg(II) concentration of 20 μg L^{-1}. Then, the mixtures were shaken at 200 rpm for 24 h to reach equilibrium, obtaining the PM-Hg(II) suspensions. For each treatment, six replicates were prepared to 1) characterize Hg(II) sorption onto particles by analyzing the THg and Hg_D in suspensions, and 2) determine the bioavailability of Hg_P using the above-mentioned biosensor. The THg concentration of one aliquot (200 μL) was analyzed using a direct mercury analyzer (DMA-80, Milestone, Italy). The remaining aliquots were filtered through a 0.22 μm filter or 3 kDa ultrafiltration tube, oxidized with BrCl (5% v/v) overnight, and analyzed for Hg_D using cold-vapor atomic fluorescence spectrometry (CVAFS, Polytech, Beijing, China). Thus, the sorption amount was calculated by the difference between THg and Hg_D (Hg_P = THg − Hg_D). The experimental procedures and conditions were similar to those of the oxic Hg(II) bioassays, except the biosensor cells were exposed to the PM-Hg(II) suspensions. Three control groups were used: (1) filtered river water without Hg(II); (2) particle suspension without Hg(II); and (3) filtered river water with 20 μg L^{-1} Hg(II) (particle-free control). All vials were acid-washed, dried, and heated in a furnace at 500 °C for 30 min to remove Hg prior to be used.

Evaluating Factors Affecting the Bioavailability of Particle-Bound Hg(II). To explore the factors controlling the microbial uptake of Hg_P, 13 model particles, including Fe_2O_3 (17, 40, 95, and 166 nm), Fe_3O_4 (98, 189, and 227 nm), Al_2O_3 (14, 422, and 1065 nm), and SiO_2 (16, 373, and 2703 nm), were used to test the effect of (1) oxygen, (2) particle composition, (3) particle size, (4) coating of organic matter on particles, and (5) particle concentration on the bioavailability of Hg_P. These five experiments were carried out by pre-equilibrating particles with Hg(II) for 24 h, analyzing Hg(II) sorption onto particles, and assaying the bioavailability of Hg_P using the Hg(II)-inducible biosensor *E. coli* PRL. The experimental procedures were similar to those used for PM, but the filtered river water was replaced by deoxygenated or oxic MMOPS. Unless specified, the bioavailability of Hg_P was studied at a particle concentration of 0.1 g L^{-1} and a Hg(II) concentration of 20 μg L^{-1} under anoxic conditions.

For experiment 1 (effect of oxygen), 166 nm Fe_2O_3 particle was taken as an example, and bioassays were conducted under both oxic and anoxic conditions. For experiment 2 (effect of particle composition), 166 nm Fe_2O_3, 189 nm Fe_3O_4, 422 nm Al_2O_3, and 373 nm SiO_2 were used. For experiment 3 (effect of particle size), all the 13 model particles were included. For experiment 4 (effect of coating with organic matter), two organic matter (HA and Cys)-coated particles were synthesized from 166 nm Fe_2O_3. Herein, HA and Cys were used as models of natural organic matter and low-molecular-weight ligands because they have been shown to play important roles in regulating the microbial uptake of Hg(II), and sorption/desorption behaviors of Hg(II) by particles.[12,19,46,47] Briefly, 0.25 g L^{-1} HA or 10 mM Cys were mixed with 5 g L^{-1} Fe_2O_3 particles in 1 mM NaCl solution. After shaking for 24 h, the mixtures were filtered through 0.45 μm membranes (Millipore, MA). Then, the HA- or Cys-Fe_2O_3 were washed three times with ultrapure water, gently scraped from the membranes, and oven-dried at 45 °C to constant weight. Fourier-transform infrared spectrometry demonstrated that HA[48] and Cys (www.chemicalbook.com: CAS_52-90-4) were coated onto the surface of Fe_2O_3 (Figure S3). For experiment 5 (effect of particle concentration), 166 nm Fe_2O_3 particle was used, and the bioavailability of Hg_P was studied using 0, 0.1, or 1 g L^{-1} Fe_2O_3. The luminescence in these particle suspensions without added Hg(II) was similar to the background signal (cells only) when assessed by Hg(II)-inducible (*E. coli* PRL) (Figure S4) and constitutive biosensor (*E. coli* PJL, Figure S5), suggesting that elements in these particles would not interfere with the subsequent Hg(II) bioavailability analysis.

Imaging the Interactions between Particles and Cells. Cell interactions with particles (166 nm Fe_2O_3) were directly visualized using field emission environmental scanning electron microscopy (FESEM, Quattro, Thermo Scientific, USA) coupled with an energy-dispersive X-ray spectroscopy

https://doi.org/10.1021/acs.est.1c08946
Environ. Sci. Technol. 2022, 56, 6754−6764

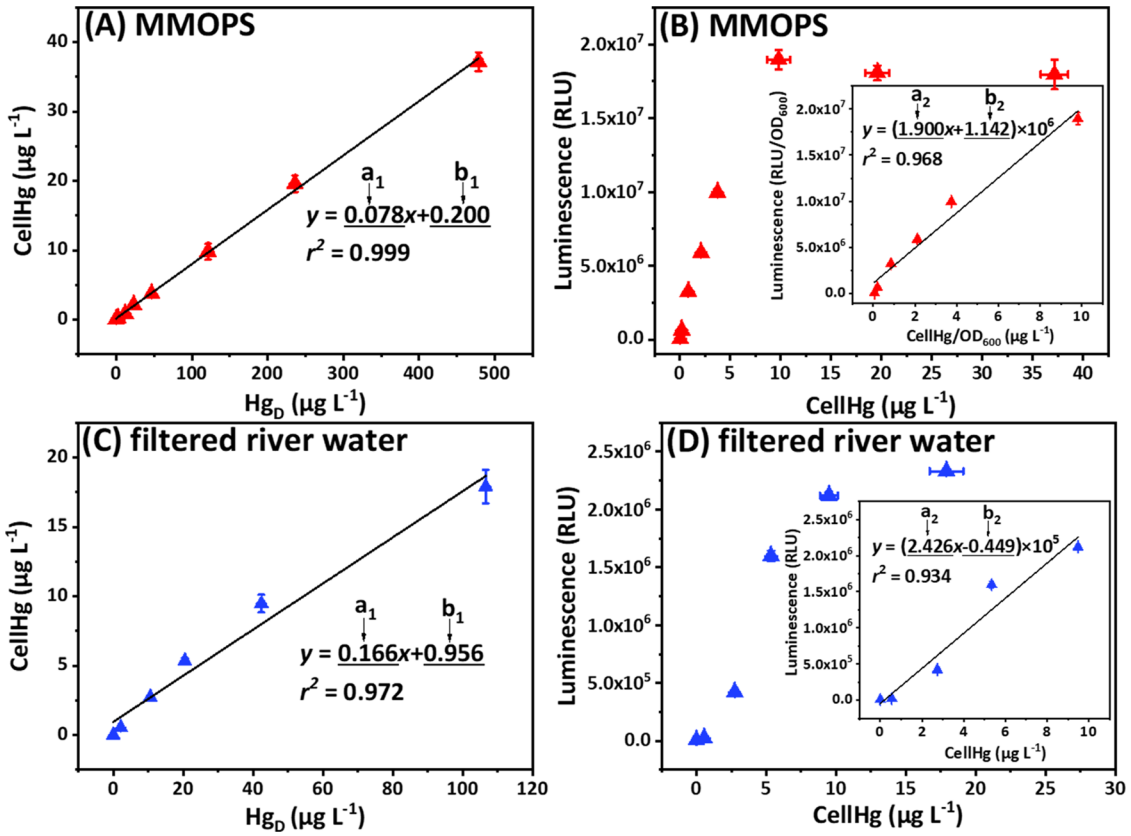

Figure 1. (A) Intracellular Hg (CellHg) versus spiked Hg(II) (Hg_D) and (B) luminescence intensity (RLU) versus CellHg ($\mu g\ L^{-1}$) of exposed to 0−200 $\mu g\ L^{-1}$ Hg(II) in culture medium (MMOPS) under anoxic conditions. (C) CellHg versus Hg_D and (D) luminescence intensity versus CellHg exposed to 0−50 $\mu g\ L^{-1}$ Hg(II) in normoxic filtered river water (CBR). Hg(II)-inducible biosensor *E. coli* PRL was used in these batch experiments. The exposure time was 3 h, and all values were normalized to OD_{600} (un-normalized raw data were present in Table S5). $CellHg_D$ can be estimated from the linear relationship between CellHg and Hg_D, with the slope (a_1) and intercept (b_1) obtained from the equations in figure (A) (MMOPS) and (C) (filtered river water). $CellHg_T$ in the presence of particles can be estimated from the linear relationship between CellHg and RLU, with slope (a_2) and intercept (b_2) obtained from the equations in figure B (MMOPS) and D (filtered river water).

(EDS). Biosensor cells (*E. coli* PRL, ~10^8 cells mL^{-1}) were mixed with 0.1 g L^{-1} particles and incubated anaerobically at 30 °C and then transferred onto a silicon wafer after 3 h. Immediately, the interactions between bacteria and particles were imaged by FESEM, and chemical compositions were analyzed using EDS. The acceleration voltage was set as 15 keV.

Calculation of Intracellular Hg. Although Hg_P is the major species in particle-Hg(II) suspension, there is still a small fraction of Hg_D. Therefore, we defined the intracellular Hg ($CellHg_T$) into two fractions according to its source: (1) intracellular Hg from Hg_D ($CellHg_D$) and (2) intracellular Hg from Hg_P ($CellHg_P$).

Assuming that the presence/absence of particles would not affect the microbial uptake of Hg_D species in suspension, $CellHg_D$ can be estimated from the linear relationship between intracellular Hg and dissolved Hg(II) concentration, with the slope (a_1) and intercept (b_1) obtained from the following equation

$$\frac{CellHg_D}{OD_{600}} = a_1 \times \frac{Hg_D}{OD_{600}} + b_1 \quad (1)$$

where Hg_D is the dissolved Hg content in suspension; $CellHg_D$ is the intracellular Hg originated from Hg_D; and OD_{600} is the absorbance value for cell suspension at 600 nm and stands for the cell density.

$CellHg_T$ in the presence of particles was estimated from the linear relationship between intracellular Hg and luminescence intensity (RLU), with slope (a_2) and intercept (b_2) obtained from the following equation

$$\frac{RLU}{OD_{600}} = a_2 \times \frac{CellHg_T}{OD_{600}} + b_2 \quad (2)$$

where RLU is the luminescence intensity of cells exposed to Hg(II); $CellHg_T$ is the intracellular total Hg. The parameters a_1, a_2, b_1, and b_2 were obtained from the Hg(II) bioassays in culture media and filtered natural water. Then, $CellHg_P$ was estimated as the difference between $CellHg_T$ and $CellHg_D$.

$$CellHg_P = CellHg_T - CellHg_D \quad (3)$$

where $CellHg_P$ is the intracellular Hg originated from particulate fraction (Hg_P).

Statistical Analysis. All statistical analyses were conducted by SPSS 19.0 software. Differences in Hg(II) bioavailability in the presence/absence of different particles throughout exposure were determined by repeated measures ANOVA (MANOVA) at a confidence interval of 95%.

RESULTS AND DISCUSSION

Biosensor Can Probe Intracellular Hg in Culture Media and Filtered Natural Water under Anoxic and Oxic Conditions. In culture media, the luminescence of the

https://doi.org/10.1021/acs.est.1c08946
Environ. Sci. Technol. 2022, 56, 6754−6764

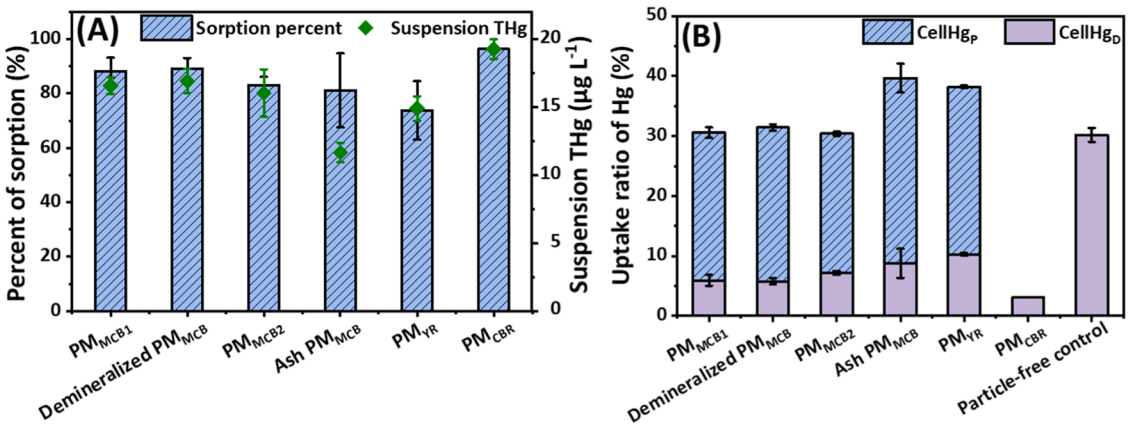

Figure 2. (A) Percent Hg(II) sorption and THg in suspension after equilibrating 0.1 g L^{-1} of particles with 20 μg L^{-1} of Hg(II) for 24 h; (B) the uptake ratio of Hg(II) (% of THg) by the Hg(II)-inducible biosensor *E. coli* PRL from Hg_P and Hg_D in suspensions. Uptake ratio of Hg = ($CellHg_P$ + $CellHg_D$)/THg in suspension. Each point represents data obtained from 3−4 replicates. Error bars represent the standard deviation.

biosensor*E. coli* PRL was rapidly induced by Hg(II), with signals detectable within 0.5 h, even at 1 μg L^{-1} Hg(II) under both anoxic and oxic conditions (Figure S6A,B). At each selected time point, the luminescence intensities linearly increased with Hg(II) concentration from 1 to 20 μg L^{-1} under both anoxic and oxic conditions (Figure S6C,D). These results were further confirmed by the intracellular Hg variation (t = 3 h) analyzed by DMPS washing and AFS detection (Figure 1). The results showed that intracellular Hg was linearly correlated with the spiked Hg(II) concentration (r^2 = 0.999, Figure 1A) and also with the luminescence intensity (r^2 = 0.968, Figure 1B). However, at higher Hg(II) concentration (>50 μg L^{-1}), the intracellular Hg was nonlinearly correlated with luminescence intensity. This may be due to the "ultimate threshold" effect of transcription activity of *mer* operon, which leads to insufficient aldehyde reductase and luciferase enzymes, limiting the luminescence emission of *E. coli* PRL.[49−51] In addition, using the constitutive biosensor *E. coli* PJL, it was found that luminescence intensity varied little when exposed to different leveled Hg(II) (0−200 μg L^{-1}) under anoxic conditions (t = 3 h, Figure S7), suggesting that the enhanced/decreased luminescence in Hg(II)-inducible biosensor *E. coli* PRL (Figures 1 and S6) was Hg(II)-dependent but not a result of cell physiology variation.[52]

Similar trends were observed for the filtered natural water under normoxic conditions, but with a lower luminescence intensity compared to culture media (Figures 1C,D, and S8). This is probably due to (1) the limited nutrients (e.g., carbon source) in river water, as evidenced by the significantly lower luminescence emitted by constitutive biosensor *E. coli* PJL in river water (CBR and YR) than that in MMOPS (Figure S9); (2) the higher levels of divalent cations in filtered river water (Table S2), which might hamper Hg(II) entering into cells. For instance, Zn(II) and Mn(II) may compete for binding sites with Hg(II) at the cell surface;[53−55] Ca(II) and Mg(II) may decrease the outer membrane permeability of bacteria;[53] and (3) alkaline pH[52] of river water (Table S2), which affect Hg(II) speciation,[56−58] particle chemistry,[59] and microbial activities,[52,60] thus controlling the Hg(II) sorption/desorption behaviors on particles and the microbial uptake process of Hg(II).

Bioavailable Hg(II), generally defined as the fraction that can cross the cell membrane,[61] induces luminescence of the Hg(II)-inducible biosensor once in the cell. Our results suggested that biosensor *E. coli* PRL can probe the bioavailable Hg(II) at environmentally relevant levels under both anoxic and oxic conditions. We found no differences in the luminescence intensity (p = 0.505, Figure S10A) or intracellular Hg (p = 0.685, Figure S10B) between anoxic and oxic exposure using the culture media. This suggests that the biosensor was effective for exploring the effect of oxygen levels on Hg(II) bioavailability. In addition, it was found that the luminescence emissions of the constitutive biosensor (*E. coli* PJL) increased linearly with OD_{600} values (Figure S11). Therefore, the OD_{600} was used as a proxy for bacterial viability, and all the data were normalized to OD_{600} so as to establish the quantitative relationship between luminescence intensity and intracellular Hg.

Hg(II) Sorbed onto Natural PM is an Important Fraction for Microbial Uptake. PM is ubiquitous in natural environments and can sorb and affect the chemical speciation of Hg(II). We first tested the bioavailability of Hg_P using a variety of natural PM. After equilibrating the PM with Hg(II) for 24 h, the THg concentrations in suspension ranged from 11.67 ± 0.72 to 19.27 ± 0.72 μg L^{-1}, with recoveries from 58 ± 3.6 to 96 ± 3.6% (Figure 2A). The loss of Hg(II) might be attributed to its reduction to elemental Hg (probably caused by the mineral-associated ferrous iron in particles)[62−64] and/or adsorption onto the container walls.[65] This would not affect the overall experiments because THg in the suspension was used in the subsequent calculations and only a portion of suspension was taken for the Hg_P bioavailability analysis.

Hg_P was the dominant Hg species in all suspensions, with percentages of Hg sorbed on particles being 88 ± 5.0% (PM_{MCB1}), 89 ± 3.7% (demineralized PM_{MCB}), 83 ± 3.2% (PM_{MCB2}), 81 ± 14% (ash PM_{MCB}), 74 ± 11% (PM_{YR}), and 96 ± 0.3% (PM_{CBR}), respectively (Figure 2A). The difference in Hg(II) sorption might be attributed to the various elemental compositions, organic matter content, or surface characteristics of particles (Tables S1 and S3). For instance, ash PM_{MCB} and PM_{YR} particles contained more inorganic minerals (e.g., Fe and Mn) and less organic matter (Table S2), which probably resulted in a lower Hg(II) sorption capacity (Figure 2A), compared with other particles.[12] These results also suggest that organic matter may play an important role in Hg(II) sorption onto particles.[12,66]

To test whether Hg_P was available for microbial uptake, the biosensor was applied to assay the bioavailability of Hg(II)

https://doi.org/10.1021/acs.est.1c08946
Environ. Sci. Technol. 2022, 56, 6754−6764

equilibrated with different types of PM for 24 h. For all of the Hg-free controls, the luminescence remained unchanged during the whole exposure (Figure S12), suggesting that the substances present in these PM did not interfere with the subsequent analysis. For particle-Hg(II) suspensions, the luminescence intensities were comparable to those of particle-free controls (Hg_D), except for PM_{CBR} (Figure S12). Estimation of $CellHg_T$ from the luminescence intensities showed that the percent uptake of Hg(II) (ratio of $CellHg_T$ to suspension THg) at 3 h varied significantly, displaying a descending trend as follows: ash PM_{MCB} (40 ± 2.9%) ≈ PM_{YR} (38 ± 1.5%) > demineralized PM_{MCB} (31 ± 2.4%) ≈ PM_{MCB1} (31 ± 1.3%) ≈ PM_{MCB2} (30 ± 1.0%) ≈ particle-free control (30 ± 1.1%) > PM_{CBR} (3.1 ± 0.0%) (repeated MANOVA, Figure 2B). Among the bioavailable Hg, 81 ± 2.9% (PM_{MCB1}), 82 ± 1.8% (demineralized PM_{MCB}), 76 ± 1.0% (PM_{MCB2}), 78 ± 6.1% (ash PM_{MCB}), and 73 ± 0.5% (PM_{YR}) of $CellHg_T$ were from the Hg_P fractions (Figure 2B), suggesting striking bioavailability of Hg_P. The presence of PM_{CBR} was in stark contrast with the others, where essentially all $CellHg_T$ were from Hg_D species in suspensions (Figure 2B), but again a very low overall bioavailable Hg fraction (3.1 ± 0.0%) needed to be noted for this type of particle. This phenomenon could be explained by the higher contents of Zn and Mn in PM_{CBR} than others (Table S3), which compete for binding sites with Hg(II) at the cell surface.[53,54,67] Besides, differences in other characteristics of PM, for example, the organic carbon (ultimately thiols),[66] may also contribute to the differences in Hg(II) bioavailability in the presence of different PM. Overall, the much higher intracellular Hg than the initial dissolved Hg content in suspensions (except for PM_{CBR}, Figure 2A) suggested that the Hg_P species were readily bioavailable; thus, the microbial uptake of PM-bound Hg(II) might be widespread in aquatic environments, with the uptake extent dependent on the nature of particles. These unusual observations suggest that the Hg_P plays a more important role in Hg biogeochemical cycle than previously recognized.[68]

Hg(II) Sorbed on Model Particles are Bioavailable under Both Oxic and Anoxic Conditions. Because the oxygen levels in water column gradually change during the settling of particles,[20,69] we assessed how the bioavailability of Hg_P was affected by oxic and anoxic conditions, taking 166 nm Fe_2O_3 as a model particle. Prior to bioavailability assays (*E. coli* PRL), Hg(II) and particles were pre-equilibrated for 24 h, so that most Hg(II) in the suspension was present in its particle-bound form (94 ± 1.3%, Figure S13A). Under oxic condition, the bioavailability of Hg(II) in the presence of particles was comparable to that of the particle-free controls ($p > 0.05$, repeated MANOVA; Figure 3), suggesting that Hg_P can be internalized by aerobes in oxic environments. Interestingly, under anoxic condition, the Hg(II) bioavailability in the presence of particles was significantly higher than those of particle-free controls and under oxic conditions ($p < 0.05$, repeated MANOVA; Figure 3). This suggests that the oxygen level of the surrounding environment is a key factor that controls the bioavailability of Hg_P. One explanation for the effects of oxygen on the microbe uptake of Hg is that bacteria may have a greater affinity for particles under anoxic condition than oxic one, probably due to the different functions of outer membrane and metal transport systems,[51,70−72] leading to stronger interactions between bacteria and Hg_P. This phenomenon was consistent with the interaction between *Shewanella oneidensis* and goethite.[72] In addition, differences in redox chemistry of particles in the presence/absence of oxygen might also contribute to the different bioavailabilities of Hg_P.

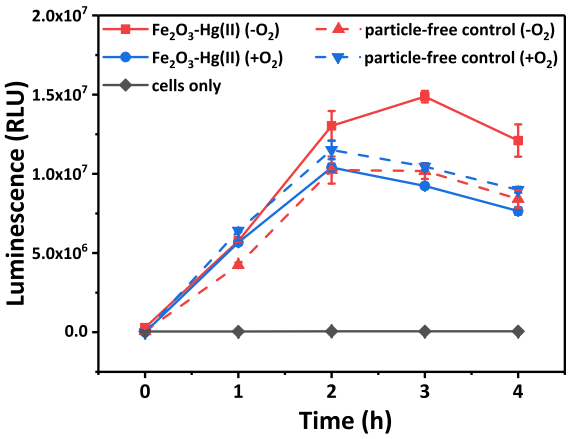

Figure 3. Bioavailability of Hg_P (166 nm Fe_2O_3) under anoxic (-O_2, red) and oxic (+O_2, blue) conditions. Hg(II)-inducible biosensor *E. coli* PRL was used in this batch experiment, and luminescence (RLU) is used as a proxy for the amount of intracellular Hg. Initial Hg(II) concentration was 20 $\mu g\ L^{-1}$, and the particle concentration was 0.1 g L^{-1}. The luminescence intensities were normalized to OD_{600} (unnormalized raw data are present in Table S6). Each data point represents data obtained from 3−4 replicates. Error bars represent the standard deviation.

The presence of particles could result in a higher local Hg(II) concentration and bacterial density on the particle surface. Therefore, bacteria were more likely to internalize Hg_P via an enhanced ligand exchange pathway due to the bacterial secretion of thiol molecules (10^7−10^8 thiols per cell).[12,18] As evidenced by the FESEM and EDS results, cells were more aggregated and were attached to the particle surfaces in the presence of Fe_2O_3 (Figure 4A−C). In contrast, cells were more

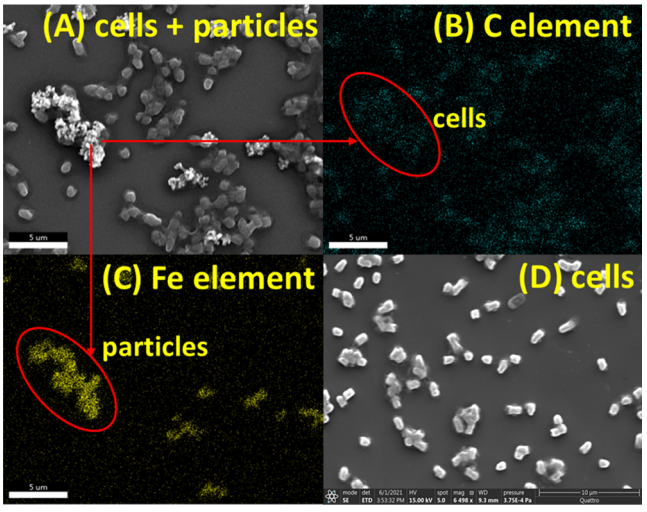

Figure 4. FESEM and EDS images for 166 nm Fe_2O_3 particles (0.1 g L^{-1}) and *E. coli* RPL cells (~10^8 cells mL^{-1}) under the anoxic condition. (A) FESEM images of cells in the presence of particles; (B) EDS mapping images of C element representing the cells in figure (A); (C) EDS mapping images of Fe element representing the particles in figure (A); and (D) FESEM images of cells in the absence of particles. The acceleration voltage was 15 keV. Samples were prepared by dropping a drop of particle-cell or cell suspension onto a silicon wafer.

https://doi.org/10.1021/acs.est.1c08946
Environ. Sci. Technol. 2022, 56, 6754−6764

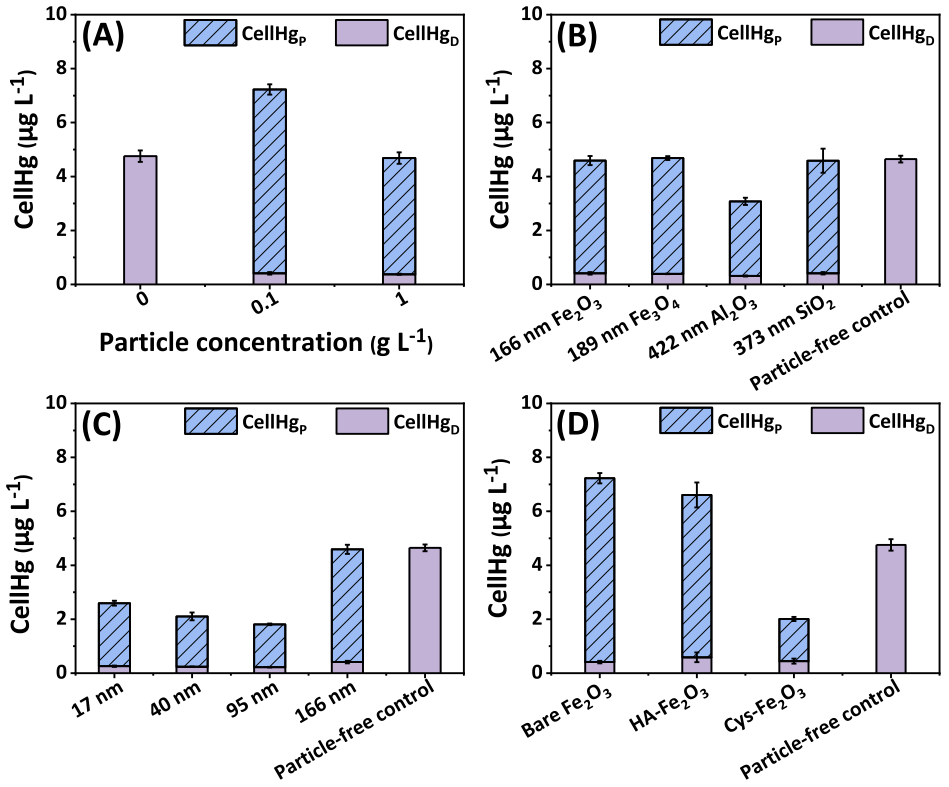

Figure 5. Factors affecting the microbial uptake of Hg(II) in the presence of various particles including (A) particle concentration (0, 0.1, and 1 g L^{-1} 166 nm Fe_2O_3); (B) particle type (Fe_2O_3, Fe_3O_4, Al_2O_3, and SiO_2); (C) particle size (17, 40, 95, and 166 nm Fe_2O_3); and (D) organic coatings (HA- and Cys-Fe_2O_3). Bare Fe_2O_3 is the uncoated 166 nm Fe_2O_3. CellHg (y-axis) is the total intracellular Hg concentration (μg L^{-1}); $CellHg_P$ (blue bars) and $CellHg_D$ (purple bars) are the intracellular Hg fractions originated from the particulate (Hg_P) and dissolved Hg(II) (Hg_D) in suspension, respectively. Hg(II)-inducible biosensor *E. coli* PRL was used in these batch tests, and experiments were conducted under anoxic conditions (t = 3 h). The initial Hg(II) concentration was 20 μg L^{-1}. Unless specified, the particle concentration was 0.1 g L^{-1}. Each point represents data obtained from 3−4 replicates. Error bars represent the standard deviation.

dispersed in the particle-free control (Figure S4D). At 3 h of anoxic exposure, the estimated $CellHg_T$ for cells exposed to Fe_2O_3-bound Hg(II) (0.1 g L^{-1} particle concentration) was 7.23 ± 0.16 μg L^{-1}, equivalent to 36 ± 0.8% of THg in suspension (Figures 5A and S14A), which was significantly higher than the initial Hg_D percent (6.0 ± 1.3%) in suspension (Figure S13). These results support the conclusion that bacteria can internalize Hg_P directly from particles, rather than from the solution after Hg(II) desorption.[12] In addition, the bioavailability of Hg_P decreased upon increasing the particle concentration from 0.1 to 1 g L^{-1} (Figures 5A and S14A) at fixed initial Hg(II) and bacterial concentrations. Thus, it is reasonable to conclude that increasing the particle concentration decreased the amount of adsorbed Hg(II) per particle, which reduced interactions between cells and Hg(II).

Microbial Uptake of Particle-Bound Hg(II) is Ubiquitous for Various Model Particles. The bioavailability of Hg_P was further assayed using three model particles, including Fe_3O_4 (189 nm), Al_2O_3 (422 nm), and SiO_2 (373 nm). After equilibrating for 24 h, 93 ± 0.2 to 96 ± 0.6% of Hg(II) in suspensions were present in its particle-bound form (Figure S13). Similar to Fe_2O_3, biosensor luminescence (*E. coli* PRL) was significantly induced by Hg_P on Fe_3O_4, Al_2O_3, and SiO_2 particles (Figure S14B). Because these particles are commonly found in aquatic environments,[73−75] these data further supported the above observation that the microbial uptake of Hg_P is widespread in natural aquatic environments.

Statistical analysis (repeated MANOVA) showed that the bioavailability of Hg_P varied significantly among different particles, displaying an trend of Fe_2O_3 ($p < 0.05$) > particle-free control ($p > 0.05$) ≈ Fe_3O_4 ($p > 0.05$) ≈ SiO_2 ($p < 0.05$) > Al_2O_3. At 3 h, the $CellHg_T$ concentrations in the presence of Fe_2O_3, Fe_3O_4, and SiO_2 were 4.59 ± 0.17, 4.68 ± 0.07, and 4.59 ± 0.44 μg L^{-1}, which were comparable to that of particle-free control (4.65 ± 0.13 μg L^{-1}) (Figure 5B); however, it was significantly lower for Al_2O_3 (3.08 ± 0.13 μg L^{-1}), possibly due to the selective bacterial recognition of mineral surfaces. For example, Fe_2O_3-coated glass adhered more bacterial cells (including *E. coli*) than that of the Al_2O_3-coated glass;[76,77] *S. oneidensis* interacted more closely with goethite (α-FeOOH) than diaspore (α-AlOOH), as evidenced by biological force microscopy.[78] This difference is reasonable considering that bacteria have a greater affinity for particle that can provide nutrition (e.g., Fe) for their growth.[78,79] Generally, bacteria produce siderophores, for example, anaerobic biosynthesis of enterobactin in *E. coli*,[80] to dissolve iron in iron oxide minerals, which enhances the influx of iron nutrients.[72,80,81] In addition, differences in particle size, surface charge (Table S4), and functional group on particle surfaces could also affect the bioavailability of Hg(II) sorbed onto various particles. These data also support the above observations that the Hg_P of ash PM_{MCB} and PM_{YR} containing higher iron levels had a greater bioavailability than other PM.

Hg(II) Sorbed on Different-Sized Particles are Available for Microbial Uptake. We further assayed the

https://doi.org/10.1021/acs.est.1c08946
Environ. Sci. Technol. 2022, 56, 6754−6764

effects of particle size on the bioavailability of Hg_P using 17, 40, 95, and 166 nm Fe_2O_3. After pre-equilibrating for 24 h, 94 ± 1.3 to 99 ± 1.3% of Hg(II) in suspensions was present in its particle-bound form (Figure S13). Similar to the 166 nm Fe_2O_3 and particle-free control, biosensor luminescence (*E. coli* PRL) was rapidly induced by Hg_P using 17, 40, and 95 nm Fe_2O_3 under anoxic conditions (Figure S14C), while the intensities were significantly lower, displaying a trend of 166 nm > particle-free control >17 > 40 > 95 nm ($p < 0.05$, repeated MANOVA). $CellHg_T$ at 3 h in the presence of 166 nm Fe_2O_3 was 4.59 ± 0.17 $\mu g\ L^{-1}$ (uptake ratio: 23 ± 0.8%), which was 1.79, 2.24, and 2.63 times higher than that of 17 (2.59 ± 0.09 $\mu g\ L^{-1}$), 40 (2.10 ± 0.15 $\mu g\ L^{-1}$), and 95 nm (1.81 ± 0.03 $\mu g\ L^{-1}$) Fe_2O_3 (Figure 5C). Similarly, the Hg_P of Fe_3O_4, Al_2O_3, and SiO_2 with different particle sizes was also available for microbial uptake, but it varied depending on the particle size (Figure S15). These results suggest that Hg_P could be internalized by microbes at all particle sizes tested although the bioavailability of Hg_P was affected by the particle size. The effect of particle size could be attributed to the different interactions between bacteria and particles of different sizes.[82] For instance, 17 nm Fe_2O_3 was in the range of 8.4−29.2 nm. As previously suggested, particles smaller than 10 nm can penetrate the outer cell wall of bacteria,[82] acting as shuttles to deliver sorbed Hg(II) into cells. For larger particles, however, Hg_P could enter cells via ligand exchange as mentioned above. In addition, the different specific surface areas of particles, which affects its Hg(II) sorption behaviors,[83,84] might also contribute to the differences in Hg_P bioavailability with different sizes. Further studies are needed to explore the mechanisms involved in the interaction between bacteria and different-sized particles to clarify the particle size-dependent internalization of Hg_P in aquatic environments.

Coating with Organic Matter Reduces the Bioavailability of Particle-Bound Hg(II). In natural environments, particles are generally coated with organic matter, changing the surface functional groups and, thus, affecting the sorption/desorption behavior of Hg(II).[10,12] To investigate how coatings with organic matter on particles affect the microbial uptake of Hg_P, we explored the bioavailability of Hg_P using the synthesized HA- and Cys-Fe_2O_3 (166 nm) particles. Whether coated with HA or Cys, the bioavailability of Hg_P was lower than that of bare Fe_2O_3 (uncoated 166 nm Fe_2O_3) under anoxic conditions ($p < 0.05$, repeated MANOVA; Figure S14D). Nevertheless, the Hg_P of HA-Fe_2O_3 displayed significantly higher bioavailability than that of the particle-free control ($p < 0.05$, repeated MANOVA; Figure S14D). Accordingly, at 3 h, $CellHg_T$ in the presence of bare Fe_2O_3 was 7.23 ± 0.16 $\mu g\ L^{-1}$, which decreased to 6.61 ± 0.38 and 2.01 ± 0.06 $\mu g\ L^{-1}$ for HA- and Cys-Fe_2O_3, respectively (Figure 5D).

Two mechanisms may be responsible for the decreased bioavailability of Hg_P with coating of organic matter: (1) organic coatings on particle surface enhanced the binding strength of Hg(II) to particles, making it harder for bacteria to compete for Hg(II) sorbed onto particles. This is partially supported by the finding that Cys has stronger Hg(II) complexation than HA,[66,85] and thus, the microbial uptake of Hg(II) from Cys-Fe_2O_3 was much lower than that from HA-Fe_2O_3 (Figures 5D and S14D). In addition, the significantly decreased bioavailability of Hg(II) sorbed on iron sulfide nanoparticles, through chemisorption of Hg(II) or formation of inert Hg sulfide, can also support this finding;[86] (2) coatings with HA or Cys limited the adhesion of bacteria onto particles, due to the electrostatic repulsion-enhanced dispersion of particles.[87−89] This hypothesis was in line with the more negative charge and the smaller hydrodynamic diameters of HA- and Cys-Fe_2O_3 than the bare ones (Table S4). Overall, these results suggested that organic coatings on particle surface significantly affect the bioavailability of Hg(II), which can partially explain the significantly lower bioavailability of Hg_P for PM_{CBR} than PM_{YR} (Figures 2B and S12B).

Environmental Implications. We developed a new approach based on a Hg(II)-inducible (*E. coli* PRL) and constitutive (*E. coli* PJL) whole-cell biosensor to evaluate how particles affect the Hg(II) bioavailability to bacteria. This approach makes it possible to trace the contribution of particle-bound Hg(II) to intracellular Hg in real-time without tedious additional treatments [e.g., separation of microbes and particles, and elution of microbial adsorbed Hg(II)]. Assaying the Hg_P bioavailability of natural and model particles demonstrated that the microbial uptake of Hg_P was ubiquitous in aquatic environments. Because Hg_P was previously recognized as an inert Hg species that could not be internalized by microorganisms, this novel finding has a significant implication on the bioavailability of Hg in the water column, sediment, and soil. The bioavailability of Hg_P in the environment can be controlled by a variety of particle characteristics, including their composition, size, and surface coating. In aquatic environment, PM has great spatial and temporal heterogeneity, which will thus greatly affect the bioavailability of Hg(II). In addition, we showed that Hg_P may be an important Hg(II) source for microbes in both oxic and anoxic environments, with enhanced bioavailability under anoxic conditions. This observation is significant for the probing Hg biogeochemical cycle in oxygen-gradient aquatic environments, especially for stratified lakes, reservoirs, and oceans. In oxic surface water, Hg_P could be internalized and reduced to elemental Hg by aerobic Hg reducers (e.g., *merA*-carrying microbes), decreasing Hg levels in aquatic systems; however, upon the settlement of particles, Hg_P could be internalized by the dominant anaerobes (including Hg methylators) on the particles, increasing MeHg formation and thus the risk of Hg to aquatic food webs. Overall, our findings help explain why settling particles have an enhanced Hg-methylation potential in aquatic systems. In addition, our data shed light on the enhanced MeHg production in sediments, where particle-bound Hg(II) is an important Hg(II) species in anoxic porewater.

■ ASSOCIATED CONTENT

Supporting Information

The Supporting Information is available free of charge at https://pubs.acs.org/doi/10.1021/acs.est.1c08946.

Additional descriptions of methods for the extraction and characterization of PM; preparation of media; characteristics of natural PM, model mineral particles, and filtered river water; scheme of Hg_P bioavailability analysis; background luminescence of model mineral particles; luminescence and growth curves of Hg(II)-inducible and constitutive biosensor in response with Hg(II) in MMOPS and filtered river water; differences in luminescence and intracellular Hg of Hg(II)-inducible biosensor between anoxic and oxic conditions; relationship between luminescence and OD_{600} of the constitutive biosensor; bioavailability of Hg_P of natural PM

https://doi.org/10.1021/acs.est.1c08946
Environ. Sci. Technol. 2022, 56, 6754−6764

and model mineral particles; and Hg(II) sorption by model mineral particles (PDF)

Intracellular Hg (CellHg) versus spiked Hg(II) (Hg_D) and RLU versus CellHg; bioavailability of Hg_P; differences in luminescence intensity and intracellular Hg of Hg(II)-inducible biosensor *E. coli* PRL between anoxic and oxic conditions; bioavailability of PM-bound Hg(II) measured as RLU over time; factors affecting the microbial uptake of Hg(II) in the presence of particles; and bioavailability of Hg_P onto model particles with different sizes under anoxic conditions (XLSX)

AUTHOR INFORMATION

Corresponding Author

Yongguang Yin − *Laboratory of Environmental Nanotechnology and Health Effect and State Key Laboratory of Environmental Chemistry and Ecotoxicology, Research Center for Eco-Environmental Sciences, Chinese Academy of Sciences, Beijing 100085, China; University of Chinese Academy of Sciences, Beijing 100049, China; Institute of Environment, Hangzhou Institute for Advanced Study, UCAS, Hangzhou 310024, China;* orcid.org/0000-0001-9392-6256; Phone: 86-10-62841180; Email: ygyin@rcees.ac.cn

Authors

Yuping Xiang − *Laboratory of Environmental Nanotechnology and Health Effect and State Key Laboratory of Environmental Chemistry and Ecotoxicology, Research Center for Eco-Environmental Sciences, Chinese Academy of Sciences, Beijing 100085, China; University of Chinese Academy of Sciences, Beijing 100049, China*

Yingying Guo − *Laboratory of Environmental Nanotechnology and Health Effect and State Key Laboratory of Environmental Chemistry and Ecotoxicology, Research Center for Eco-Environmental Sciences, Chinese Academy of Sciences, Beijing 100085, China; University of Chinese Academy of Sciences, Beijing 100049, China*

Guangliang Liu − *Department of Chemistry and Biochemistry, Florida International University, Miami, Florida 33199, United States; Institute of Environment and Health, Jianghan University, Wuhan 430056, China;* orcid.org/0000-0003-4248-1167

Yanwei Liu − *Laboratory of Environmental Nanotechnology and Health Effect and State Key Laboratory of Environmental Chemistry and Ecotoxicology, Research Center for Eco-Environmental Sciences, Chinese Academy of Sciences, Beijing 100085, China; University of Chinese Academy of Sciences, Beijing 100049, China*

Maoyong Song − *Laboratory of Environmental Nanotechnology and Health Effect, Research Center for Eco-Environmental Sciences, Chinese Academy of Sciences, Beijing 100085, China*

Jianbo Shi − *State Key Laboratory of Environmental Chemistry and Ecotoxicology, Research Center for Eco-Environmental Sciences, Chinese Academy of Sciences, Beijing 100085, China;* orcid.org/0000-0003-2637-1929

Ligang Hu − *State Key Laboratory of Environmental Chemistry and Ecotoxicology, Research Center for Eco-Environmental Sciences, Chinese Academy of Sciences, Beijing 100085, China;* orcid.org/0000-0002-6213-4720

Yong Cai − *Laboratory of Environmental Nanotechnology and Health Effect and State Key Laboratory of Environmental Chemistry and Ecotoxicology, Research Center for Eco-Environmental Sciences, Chinese Academy of Sciences, Beijing 100085, China; Department of Chemistry and Biochemistry, Florida International University, Miami, Florida 33199, United States;* orcid.org/0000-0002-2811-4638

Guibin Jiang − *State Key Laboratory of Environmental Chemistry and Ecotoxicology, Research Center for Eco-Environmental Sciences, Chinese Academy of Sciences, Beijing 100085, China;* orcid.org/0000-0002-6335-3917

Complete contact information is available at: https://pubs.acs.org/10.1021/acs.est.1c08946

Notes

The authors declare no competing financial interest.

ACKNOWLEDGMENTS

This work was supported by the National Natural Science Foundation of Shandong (ZR2020ZD20), National Natural Science Foundation of China (22006151, 21777178, and 21976193), and Strategic Priority Research Program of the Chinese Academy of Sciences (XDPB2005). Y.Y. acknowledges supports from National Young Top-Notch Talents (W03070030) and Youth Innovation Promotion Association of the Chinese Academy of Sciences (Y202011).

REFERENCES

(1) UNEP. *Global Mercury Assessment: Sources, Emissions, Releases and Environmental Transport*; UNEP Chemicals Branch: Geneva, Switzerland, 2013.

(2) Ullrich, S. M.; Tanton, T. W.; Abdrashitova, S. A. Mercury in the aquatic environment: A review of factors affecting methylation. *Crit. Rev. Environ. Sci. Technol.* **2001**, *31*, 241−293.

(3) Paranjape, A. R.; Hall, B. D. Recent advances in the study of mercury methylation in aquatic systems. *Facets* **2017**, *2*, 85−119.

(4) Gilmour, C. C.; Podar, M.; Bullock, A. L.; Graham, A. M.; Brown, S. D.; Somenahally, A. C.; Johs, A.; Hurt, R. A., Jr.; Bailey, K. L.; Elias, D. A. Mercury methylation by novel microorganisms from new environments. *Environ. Sci. Technol.* **2013**, *47*, 11810−11820.

(5) Parks, J. M.; Johs, A.; Podar, M.; Bridou, R.; Hurt, R. A., Jr.; Smith, S. D.; Tomanicek, S. J.; Qian, Y.; Brown, S. D.; Brandt, C. C.; Palumbo, A. V.; Smith, J. C.; Wall, J. D.; Elias, D. A.; Liang, L. The genetic basis for bacterial mercury methylation. *Science* **2013**, *339*, 1332−1335.

(6) Mathema, V. B.; Thakuri, B. C.; Sillanpää, M. Bacterial mer operon-mediated detoxification of mercurial compounds: A short review. *Arch. Microbiol.* **2011**, *193*, 837−844.

(7) Hsu-Kim, H.; Kucharzyk, K. H.; Zhang, T.; Deshusses, M. A. Mechanisms regulating mercury bioavailability for methylating microorganisms in the aquatic environment: A critical review. *Environ. Sci. Technol.* **2013**, *47*, 2441−2456.

(8) Lin, C. C.; Yee, N.; Barkay, T. Microbial transformations in the mercury cycle. In *Environmental Chemistry and Toxicology of Mercury*; Liu, G., Cai, Y., O'Driscoll, N., Eds.; John Wiley & Sons, Inc.: Hoboken, New Jersey, 2012; pp 155−191.

(9) Ndu, U.; Mason, R. P.; Zhang, H.; Lin, S.; Visscher, P. T. Effect of inorganic and organic ligands on the bioavailability of methylmercury as determined by using a mer-lux bioreporter. *Appl. Environ. Microbiol.* **2012**, *78*, 7276−7282.

(10) Chiasson-Gould, S. A.; Blais, J. M.; Poulain, A. J. Dissolved organic matter kinetically controls mercury bioavailability to bacteria. *Environ. Sci. Technol.* **2014**, *48*, 3153−3161.

(11) Jonsson, S.; Skyllberg, U.; Nilsson, M. B.; Lundberg, E.; Andersson, A.; Björn, E. Differentiated availability of geochemical mercury pools controls methylmercury levels in estuarine sediment and biota. *Nat. Commun.* **2014**, *5*, 4624.

(12) Zhang, L.; Wu, S.; Zhao, L.; Lu, X.; Pierce, E. M.; Gu, B. Mercury sorption and desorption on organo-mineral particulates as a source for microbial methylation. *Environ. Sci. Technol.* **2019**, *53*, 2426−2433.
(13) Gu, B.; Mishra, B.; Miller, C.; Wang, W.; Lai, B.; Brooks, S. C.; Kemner, K. M.; Liang, L. X-ray fluorescence mapping of mercury on suspended mineral particles and diatoms in a contaminated freshwater system. *Biogeosciences* **2014**, *11*, 5259−5267.
(14) Balogh, S. J.; Swain, E. B.; Nollet, Y. H. Characteristics of mercury speciation in Minnesota rivers and streams. *Environ. Pollut.* **2008**, *154*, 3−11.
(15) Xu, J.; Bland, G. D.; Gu, Y.; Ziaei, H.; Xiao, X.; Deonarine, A.; Reible, D.; Bireta, P.; Hoelen, T. P.; Lowry, G. V. Impacts of sediment particle grain size and mercury speciation on mercury bioavailability potential. *Environ. Sci. Technol.* **2021**, *55*, 12393−12402.
(16) Choe, K.-Y.; Gill, G. A.; Lehman, R. Distribution of particulate, colloidal, and dissolved mercury in San Francisco Bay estuary. 1. Total mercury. *Limnol. Oceanogr.* **2003**, *48*, 1535−1546.
(17) Hintelmann, H.; Keppeljones, K.; Evans, R. D. Constants of mercury methylation and demethylation rates in sediments and comparison of tracer and ambient mercury availability. *Environ. Toxicol. Chem.* **2000**, *19*, 2204−2211.
(18) Zhao, L.; Li, Y.; Zhang, L.; Zheng, J.; Pierce, E. M.; Gu, B. Mercury adsorption on minerals and its effect on microbial methylation. *ACS Earth Space Chem.* **2019**, *3*, 1338−1345.
(19) Zhang, L.; Wu, S.; Zhao, L.; Lu, X.; Pierce, E. M.; Gu, B. Mercury sorption and desorption on organo-mineral particulates as a source for microbial methylation. *Environ. Sci. Technol.* **2019**, *53*, 2426−2433.
(20) Diez, E. G.; Loizeau, J. L.; Cosio, C.; Bouchet, S.; Adatte, T.; Amouroux, D.; Bravo, A. G. Role of settling particles on mercury methylation in the oxic water column of freshwater systems. *Environ. Sci. Technol.* **2016**, *50*, 11672.
(21) Weltje, G. J.; Tjallingii, R. Calibration of xrf core scanners for quantitative geochemical logging of sediment cores: Theory and application. *Earth Planet. Sci. Lett.* **2008**, *274*, 423−438.
(22) Cossa, D.; Averty, B.; Pirrone, N. The origin of methylmercury in open mediterranean waters. *Limnol. Oceanogr.* **2009**, *54*, 837−844.
(23) Sunderland, E. M.; Krabbenhoft, D. P.; Moreau, J. W.; Strode, S. A.; Landing, W. M. Mercury sources, distribution, and bioavailability in the north Pacific Ocean: Insights from data and models. *Global Biogeochem. Cycles* **2009**, *23*, GB2010.
(24) Ortiz, V. L.; Mason, R. P.; Evan Ward, J. An examination of the factors influencing mercury and methylmercury particulate distributions, methylation and demethylation rates in laboratory-generated marine snow. *Mar. Chem.* **2015**, *177*, 753−762.
(25) Capo, E.; Bravo, A. G.; Soerensen, A. L.; Bertilsson, S.; Pinhassi, J.; Feng, C.; Andersson, A. F.; Buck, M.; Björn, E. *Deltaproteobacteria* and *spirochaetes*-like bacteria are abundant putative mercury methylators in oxygen-deficient water and marine particles in the Baltic sea. *Front. Microbiol.* **2020**, *11*, 574080.
(26) Lamborg, C. H.; Hammerschmidt, C. R.; Bowman, K. L. An examination of the role of particles in oceanic mercury cycling. *Philos. Trans. R. Soc., A* **2016**, *374*, 20150297.
(27) Schaefer, J. K.; Rocks, S. S.; Zheng, W.; Liang, L.; Gu, B.; Morel, F. M. M. Active transport, substrate specificity, and methylation of Hg(II) in anaerobic bacteria. *Proc. Natl. Acad. Sci. U.S.A.* **2011**, *108*, 8714−8719.
(28) Liu, Y.-R.; Lu, X.; Zhao, L.; An, J.; He, J.Z.; Pierce, E. M.; Johs, A.; Gu, B. Effects of cellular sorption on mercury bioavailability and methylmercury production by *Desulfovibrio desulfuricans* ND132. *Environ. Sci. Technol.* **2016**, *50*, 13335−13341.
(29) Lu, X.; Johs, A.; Zhao, L.; Wang, L.; Pierce, E. M.; Gu, B. Nanomolar copper enhances mercury methylation by *Desulfovibrio desulfuricans* ND132. *Environ. Sci. Technol. Lett.* **2018**, *5*, 372−376.
(30) Thomas, S. A.; Rodby, K. E.; Roth, E. W.; Wu, J.; Gaillard, J.-F. Spectroscopic and Microscopic Evidence of Biomediated HgS Species Formation from Hg(II)-Cysteine Complexes: Implications for Hg(II) Bioavailability. *Environ. Sci. Technol.* **2018**, *52*, 10030−10039.
(31) Bolea, E.; Jiménez-Lamana, J.; Laborda, F.; Abad-Álvaro, I.; Bladé, C.; Arola, J. R. Detection and characterization of silver nanoparticles and dissolved species of silver in culture medium and cells by AsFlFFF-UV-Vis-ICPMS: Application to nanotoxicity tests. *Analyst* **2014**, *139*, 914−922.
(32) Ndu, U.; Christensen, G. A.; Rivera, N. A.; Gionfriddo, C. M.; Deshusses, M. A.; Elias, D. A.; Hsu-Kim, H. Quantification of mercury bioavailability for methylation using diffusive gradient in thin-film samplers. *Environ. Sci. Technol.* **2018**, *52*, 8521−8529.
(33) Tang, W.L.; Liu, Y.R.; Guan, W.Y.; Zhong, H.; Qu, X.M.; Zhang, T. Understanding mercury methylation in the changing environment: Recent advances in assessing microbial methylators and mercury bioavailability. *Sci. Total Environ.* **2020**, *714*, 136827.
(34) Stenzler, B.; Hinz, A.; Ruuskanen, M.; Poulain, A. J. Ionic strength differentially affects the bioavailability of neutral and negatively charged inorganic Hg complexes. *Environ. Sci. Technol.* **2017**, *51*, 9653−9662.
(35) Rasmussen, L. D.; Sørensen, S. J.; Turner, R. R.; Barkay, T. Application of a mer-lux biosensor for estimating bioavailable mercury in soil. *Soil Biol. Biochem.* **2000**, *32*, 639−646.
(36) Ndu, U.; Barkay, T.; Mason, R. P.; Schartup, A. T.; Al-Farawati, R.; Liu, J.; Reinfelder, J. R. The use of a mercury biosensor to evaluate the bioavailability of mercury-thiol complexes and mechanisms of mercury uptake in bacteria. *PLoS One* **2015**, *10*, No. e0138333.
(37) Mangal, V.; Stenzler, B. R.; Poulain, A. J.; Guéguen, C. Aerobic and anaerobic bacterial mercury uptake is driven by algal organic matter composition and molecular weight. *Environ. Sci. Technol.* **2019**, *53*, 157−165.
(38) Selifonova, O.; Burlage, R.; Barkay, T. Bioluminescent sensors for detection of bioavailable Hg(II) in the environment. *Appl. Environ. Microbiol.* **1993**, *59*, 3083−3090.
(39) Huang, Y.-N.; Qian, T.-T.; Dang, F.; Yin, Y.-G.; Li, M.; Zhou, D.-M. Significant contribution of metastable particulate organic matter to natural formation of silver nanoparticles in soils. *Nat. Commun.* **2019**, *10*, 3775.
(40) Stenzler, B. R.; Gaudet, J.; Poulain, A. J. An anaerobic biosensor assay for the detection of mercury and cadmium. *J. Visualized Exp.* **2018**, *142*, No. e58324.
(41) Kelly, C. A.; Rudd, J. W. M.; Holoka, M. H. Effect of pH on mercury uptake by an aquatic bacterium: Implications for Hg cycling. *Environ. Sci. Technol.* **2003**, *37*, 2941−2946.
(42) Golding, G. R.; Kelly, C. A.; Sparling, R.; Loewen, P. C.; Rudd, J. W. M.; Barkay, T. Evidence for facilitated uptake of Hg(II) by *vibrio anguillarum* and *Escherichia coli* under anaerobic and aerobic conditions. *Limnol. Oceanogr.* **2002**, *47*, 967−975.
(43) Barkay, T.; Gillman, M.; Turner, R. R. Effects of dissolved organic carbon and salinity on bioavailability of mercury. *Appl. Environ. Microbiol.* **1997**, *63*, 4267−4271.
(44) Phillips-Jones, M. K. Bioluminescence (lux) expression in the anaerobeClostridium perfringens. *FEMS Microbiol. Lett.* **1993**, *106*, 265−270.
(45) Ribeiro, R. F. L.; Germano, A. Development and validation of a method for the determination of Hg in animal tissues (equine muscle, bovine kidney and swine kidney, and poultry muscle) by direct mercury analysis (DMA). *Microchem. J.* **2015**, *121*, 237−243.
(46) Graham, A. M.; Aiken, G. R.; Gilmour, C. C. Dissolved organic matter enhances microbial mercury methylation under sulfidic conditions. *Environ. Sci. Technol.* **2012**, *46*, 2715−2723.
(47) Thomas, S. A.; Catty, P.; Hazemann, J.-L.; Michaud-Soret, I.; Gaillard, J.-F. The role of cysteine and sulfide in the interplay between microbial Hg(II) uptake and sulfur metabolism. *Metallomics* **2019**, *11*, 1219−1229.
(48) Yang, T.; Hodson, M. E. The copper complexation ability of a synthetic humic-like acid formed by an abiotic humification process and the effect of experimental factors on its copper complexation ability. *Environ. Sci. Pollut. Res. Int.* **2018**, *25*, 15873−15884.
(49) Ralston, D. M.; O'Halloran, T. V. Ultrasensitivity and heavy-metal selectivity of the allosterically modulated MerR transcription complex. *Proc. Natl. Acad. Sci. U.S.A.* **1990**, *87*, 3846−3850.

https://doi.org/10.1021/acs.est.1c08946
Environ. Sci. Technol. 2022, 56, 6754−6764

(50) O'Halloran, T. V.; Frantz, B.; Shin, M. K.; Ralston, D. M.; Wright, J. G. The MerR heavy metal receptor mediates positive activation in a topologically novel transcription complex. *Cell* **1989**, *56*, 119−129.
(51) Golding, G. The Effect of Various Physiological Conditions on Hg(II) Uptake in *Escherichia coli* and *vibrio Anguillarum*. Ph.D. Dissertation, University of Manitoba, Winnipeg, Canada, 2005.
(52) Golding, G. R.; Sparling, R.; Kelly, C. A. Effect of pH on Intracellular Accumulation of Trace Concentrations of Hg(II) in Escherichia coli under Anaerobic Conditions, as Measured Using a mer-lux Bioreporter. *Appl. Environ. Microbiol.* **2008**, *74*, 667−675.
(53) Daguené, V.; McFall, E.; Yumvihoze, E.; Xiang, S.; Amyot, M.; Poulain, A. J. Divalent Base Cations Hamper Hg^{II} Uptake. *Environ. Sci. Technol.* **2012**, *46*, 6645−6653.
(54) Schaefer, J. K.; Szczuka, A.; Morel, F. M. M. Effect of divalent metals on Hg(II) uptake and methylation by bacteria. *Environ. Sci. Technol.* **2014**, *48*, 3007−3013.
(55) Porcheron, G.; Garénaux, A.; Proulx, J.; Sabri, M.; Dozois, C. M. Iron, copper, zinc, and manganese transport and regulation in pathogenic enterobacteria: Correlations between strains, site of infection and the relative importance of the different metal transport systems for virulence. *Front. Cell. Infect. Microbiol.* **2013**, *3*, 90.
(56) Barrow, N. J.; Cox, V. C. The effects of pH and chloride concentration on mercury sorption. I. By goethite. *J. Soil Sci.* **1992**, *43*, 295−304.
(57) Liu, G.; Li, Y.; Cai, Y. Adsorption of mercury on solids in the aquatic environment. In *Environmental Chemistry and Toxicology of Mercury*; Liu, G., Cai, Y., O'Driscoll, N., Eds.; John Wiley & Sons, Inc: Hoboken, New Jersey, 2012; pp 367−387.
(58) Lockwood, R. A.; Chen, K. Y. Adsorption of mercury(II) by hydrous manganese oxides. *Environ. Sci. Technol.* **1973**, *7*, 1028−1034.
(59) Lyons, J.; Furlong, D.; Healy, T. The electrical double-layer properties of the mica (muscovite)-aqueous electrolyte interface. *Aust. J. Chem.* **1981**, *34*, 1177−1187.
(60) Golding, G. R.; Kelly, C. A.; Sparling, R.; Loewen, P. C.; Barkay, T. Evaluation of mercury toxicity as a predictor of mercury bioavailability. *Environ. Sci. Technol.* **2007**, *41*, 5685−5692.
(61) Harms, H.; Wells, M. C.; van der Meer, J. R. Whole-cell living biosensors-are they ready for environmental application? *Appl. Microbiol. Biotechnol.* **2006**, *70*, 273−280.
(62) Yee, N.; Parikh, M.; Lin, C. C.; Kukkadapu, R.; Barkay, T. Reduction of Hg(II) to Hg(0) by biogenic magnetite. *Geochim. Cosmochim. Acta* **2010**, *74*, 1184.
(63) Wiatrowski, H. A.; Das, S.; Kukkadapu, R.; Ilton, E. S.; Barkay, T.; Yee, N. Reduction of Hg(II) to Hg(0) by magnetite. *Environ. Sci. Technol.* **2009**, *43*, 5307−5313.
(64) Etique, M.; Bouchet, S.; Byrne, J. M.; ThomasArrigo, L. K.; Kaegi, R.; Kretzschmar, R. Mercury reduction by nanoparticulate vivianite. *Environ. Sci. Technol.* **2021**, *55*, 3399−3407.
(65) Beneš, P.; Rajman, I. Radiochemical study of the sorption of trace elements. V. Adsorption and desorption of bivalent mercury on polyethylene. *Collect. Czech. Chem. Commun.* **1969**, *34*, 1375−1386.
(66) Ravichandran, M. Interactions between mercury and dissolved organic matter–a review. *Chemosphere* **2004**, *55*, 319−331.
(67) Szczuka, A.; Morel, F. M. M.; Schaefer, J. K. Effect of thiols, zinc, and redox conditions on Hg uptake in *Shewanella oneidensis*. *Environ. Sci. Technol.* **2015**, *49*, 7432−7438.
(68) Hintelmann, H.; Harris, R. Application of multiple stable mercury isotopes to determine the adsorption and desorption dynamics of Hg(II) and MeHg to sediments. *Mar. Chem.* **2004**, *90*, 165−173.
(69) Montgomery, S.; Lucotte, M.; Pichet, P.; Mucci, A. Total dissolved mercury in the water column of several natural and artificial aquatic systems of northern Quebec (Canada). *Can. J. Fish. Aquat. Sci.* **1995**, *52*, 2483−2492.
(70) Kehres, D. G.; Zaharik, M. L.; Finlay, B. B.; Maguire, M. E. The NRAMP proteins of *Salmonella typhimurium* and *Escherichia coli* are selective manganese transporters involved in the response to reactive oxygen. *Mol. Microbiol.* **2000**, *36*, 1085−1100.
(71) Unden, G.; Becker, S.; Bongaerts, J.; Holighaus, G.; Schirawski, J.; Six, S. O_2-sensing and O_2-dependent gene-regulation in facultatively anaerobic-bacteria. *Arch. Microbiol.* **1995**, *164*, 81−90.
(72) Lower, S. K.; Hochella, M. F.; Beveridge, T. J. Bacterial Recognition of Mineral Surfaces: Nanoscale Interactions Between Shewanella and α-FeOOH. *Science* **2001**, *292*, 1360−1363.
(73) Li, T.; Sun, G.; Yang, C.; Liang, K.; Ma, S.; Huang, L.; Luo, W. Source apportionment and source-to-sink transport of major and trace elements in coastal sediments: Combining positive matrix factorization and sediment trend analysis. *Sci. Total Environ.* **2019**, *651*, 344−356.
(74) Kansara, K.; Bolan, S.; Radhakrishnan, D.; Palanisami, T.; Al-Muhtaseb, A. a. H.; Bolan, N.; Vinu, A.; Kumar, A.; Karakoti, A. A critical review on the role of abiotic factors on the transformation, environmental identity and toxicity of engineered nanomaterials in aquatic environment. *Environ. Pollut.* **2022**, *296*, 118726.
(75) Amde, M.; Liu, J.f.; Tan, Z.Q.; Bekana, D. Transformation and bioavailability of metal oxide nanoparticles in aquatic and terrestrial environments. A review. *Environ. Pollut.* **2017**, *230*, 250−267.
(76) Vadillo-Rodríguez, V.; Logan, B. E. Localized attraction correlates with bacterial adhesion to glass and metal oxide substrata. *Environ. Sci. Technol.* **2006**, *40*, 2983−2988.
(77) Li, B.; Logan, B. E. Bacterial adhesion to glass and metal-oxide surfaces. *Colloids Surf., B* **2004**, *36*, 81−90.
(78) Kendall, T. A.; Hochella, M. F., Jr Measurement and interpretation of molecular-level forces of interaction between the siderophore azotobactin and mineral surfaces. *Geochim. Cosmochim. Acta* **2003**, *67*, 3537−3546.
(79) Appenzeller, B. M. R.; Yañez, C.; Jorand, F.; Block, J.C. Advantage provided by iron for *Escherichia coli* growth and cultivability in drinking water. *Appl. Environ. Microbiol.* **2005**, *71*, 5621−5623.
(80) Kwon, O.; Hudspeth, M. E.; Meganathan, R. Anaerobic biosynthesis of enterobactin Escherichia coli: regulation of entC gene expression and evidence against its involvement in menaquinone (vitamin K2) biosynthesis. *J. Bacteriol.* **1996**, *178*, 3252−3259.
(81) Neubauer, U.; Nowack, B.; Furrer, G.; Schulin, R. Heavy metal sorption on clay minerals affected by the siderophore desferrioxamine B. *Environ. Sci. Technol.* **2000**, *34*, 2749−2755.
(82) Dehner, C. A.; Barton, L.; Maurice, P. A.; DuBois, J. L. Size-dependent bioavailability of hematite (α-Fe_2O_3) nanoparticles to a common aerobic bacterium. *Environ. Sci. Technol.* **2011**, *45*, 977−983.
(83) Lee, J. H. Chemical Optimization of in Situ Emplacement of Nano-Particulate Iron Sulfide in Porous Media. Ph.D. Dissertation, University of Michigan, Ann Arbor, MI, 2009.
(84) Wang, M.; Li, Y.; Zhao, D.; Zhuang, L.; Yang, G.; Gong, Y. Immobilization of mercury by iron sulfide nanoparticles alters mercury speciation and microbial methylation in contaminated groundwater. *Chem. Eng. J.* **2020**, *381*, 122664.
(85) Senevirathna, W. U.; Zhang, H.; Gu, B. Effect of carboxylic and thiol ligands (oxalate, cysteine) on the kinetics of desorption of Hg(II) from kaolinite. *Water, Air, Soil Pollut.* **2011**, *215*, 573−584.
(86) Xiang, Y.; Zhu, A.; Guo, Y.; Liu, G.; Chen, B.; He, B.; Liang, Y.; Yin, Y.; Cai, Y.; Jiang, G. Decreased bioavailability of both inorganic mercury and methylmercury in anaerobic sediments by sorption on iron sulfide nanoparticles. *J. Hazard. Mater.* **2022**, *424*, 127399.
(87) Ravichandran, M.; Aiken, G. R.; Ryan, J. N.; Reddy, M. M. Inhibition of precipitation and aggregation of metacinnabar (mercuric sulfide) by dissolved organic matter isolated from the Florida Everglades. *Environ. Sci. Technol.* **1999**, *33*, 1418−1423.
(88) Li, Z.; Greden, K.; Alvarez, P. J. J.; Gregory, K. B.; Lowry, G. V. Adsorbed polymer and nom limits adhesion and toxicity of nano scale zerovalent iron to *E. coli*. *Environ. Sci. Technol.* **2010**, *44*, 3462−3467.
(89) Chekli, L.; Phuntsho, S.; Roy, M.; Shon, H. K. Characterisation of Fe-oxide nanoparticles coated with humic acid and Suwannee River natural organic matter. *Sci. Total Environ.* **2013**, *461*−*462*, 19−27.

https://doi.org/10.1021/acs.est.1c08946
Environ. Sci. Technol. 2022, 56, 6754−6764